2013 IEEE 10th International Symposium on Biomedical Imaging:
From Nano to Macro
San Francisco, CA, USA, April 7-11, 2013

AUTOMATIC NORMAL-ABNORMAL VIDEO FRAME CLASSIFICATION FOR COLONOSCOPY

Siyamalan Manivannan[⋆] *Ruixuan Wang*[⋆] *Emanuele Trucco*[⋆] *Adrian Hood*[†]

[⋆] CVIP Computer Vision and Image Processing group, School of Computing, University of Dundee, UK
[†]Leeds Institute of Molecular Medicine, University of Leeds, UK

ABSTRACT

Two novel schemes are proposed to represent intermediate-scale features for normal-abnormal classification of colonoscopy images. The first scheme works on the full-resolution image, the second on a multi-scale pyramid space. Both schemes support any feature descriptor; here we use multi-resolution local binary patterns which outperformed other features reported in the literature in our comparative experiments. We also compared experimentally two types of features not previously used in colonoscopy image classification, bag of features and sparse coding, each with and without spatial pyramid matching (SPM). We find that SPM improves performance, therefore supporting the importance of intermediate-scale features as in the proposed schemes for classification. Within normal-abnormal frame classification, we show that our representational schemes outperforms other features reported in the literature in leave-N-out tests with a database of 2100 colonoscopy images.

1. INTRODUCTION

More than one million new colorectal cancer cases are diagnosed yearly worldwide. It is the second leading cause of cancer death in the world and the third most common cancer in the UK [1]. Colonoscopy remains the gold standard for colorectal cancer screening, because of its high sensitivity ($> 90\%$) and high specificity ($> 94\%$) for small lesions (< 1.0 cm). Adenoma detection rate (ADR), in terms of lesion detection, is a surrogate marker of quality of colonoscopy [2]. A reliable image processing system detecting abnormalities (including polyps, cancer, ulcers, bleeding, tumors, and Crohn disease) in colonoscopy videos would be a useful tool in improving ADR. Here, we concentrate on normal-abnormal frame classification, a challenging task as abnormalities in colon vary in size, type, color, and shape (Figure 1).

Most work on automatic abnormality detection and frame classification for colonoscopy images analysis (henceforth CIA) applies standard classification techniques like support vector machines or artificial neural network. Various visual features are adopted, including texture, color, shape, and combinations thereof. Such features are limited in several aspects. Almost all CIA papers compute statistics of local features (e.g., local binary patterns or intensity for each pixel) over the whole image, which may fail to capture the shape or contour information which often appears at intermediate-scale image regions. Concatenated color histograms and MPEG-7 edge histograms [3] obtained from non-overlapping image regions have been used to capture intermediate-scale shape information, but they also encode spatial (location) information largely irrelevant with colonoscopy images, as lesions appear in arbitrary locations.

This paper proposes two novel representational schemes which capture statistics of *intermediate-scale* features in addition to statistics of local features, disregarding spatial information of features in the image, leading to accuracy improvements in normal-abnormal frame classification.

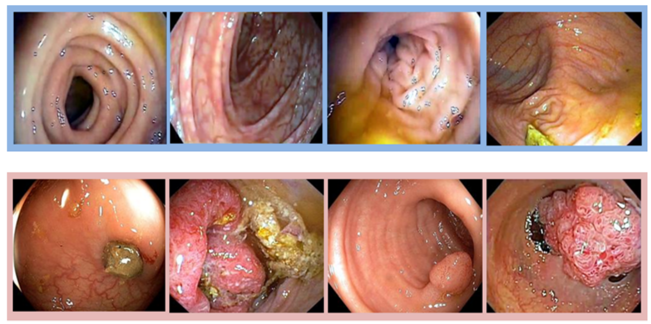

Fig. 1. Some images from our database. Top: normal images. Bottom: abnormal images.

Texture features such as those based on local binary patterns (LBP), texture spectrum (TS), and gray level co-occurrence matrices (GLCM) are used at a single resolution in the colonoscopy literature. Using a set of comparative experiments, this paper shows that multi-resolution LBP features (mLBP), providing a richer local description and reportedly robust to noise and illumination changes [4], improve performance in normal-abnormal frame classification compared to the features proposed in the literature [5, 6, 7, 8, 9, 10].

State-of-the-art feature representations developed in computer vision, such as bag of words (BOW), sparse coding (SC), and their extensions [11, 12, 13], have not been applied to CIA. This paper evaluates the performance of these schemes with a dataset of 2100 colonoscopy images. In particular, by experimentally evaluating these features with and without the integration of spatial pyramids information, additional evidence is provided that intermediate-scale feature information can improve accuracy in normal-abnormal classification. Last but not least, this paper further improves classification efficiency by a simple and efficient feature selection algorithm, the F-score.

2. RELATED WORK

Texture, color, shape, and their combinations have been used for lesion detection and frame classification in CIA.

Statistical measures (e.g., contrast, energy) from gray level co-occurrence matrices (GLCM) in frequency or spatial domain are often a basis to generate more complex texture features, although these statistics can also be directly used, e.g., for detection of precancerous polyps [5]. A widely used GLCM-based feature is color wavelet covariance (CWC) [6, 7]. In essence, entries in a CWC capture the covariance of statistical measures of co-occurrence of wavelet coefficients between color channels [6]. CWC has been used to detect polyps [6] and to classify images from wireless capsule endoscopy (WCE) into 5 different categories (normal, bleeding, ulcer, polyps and unclassified defects) [7]. CWC-related measures have been used to detect colorectal lesions [5].

Statistics of LBP (e.g., histograms) have also been used as texture features in colonosopcy image analysis. LBP [14] describes the local texture around each pixel by comparing and thresholding the neighbouring pixels with respect to the central pixel. LBP-based statistics have been used for polyp detection [15] and bleeding detection [8]. A comparative study showed that GLCM-based and LBP-based features performed equally well for polyp detection [16] . In addition, similar to LBP, texture spectra (TS) features have been used to classify WCE images [9].

Color is a salient feature for bleeding detection. Histograms or other statistics of color in different color spaces (e.g., RGB or HSV) have been reported for bleeding detection in WCE images, e.g., in [17]. Color histograms have also been used for colonoscopy frame classification, reportedly performing better than CWC features for classifying frames as informative (e.g., with folds, lumen, abnormalities) or non-informative (e.g., with poor quality due to turbidity), and as containing bleeding or not [10].

Color and texture features are often combined together for colonoscopy image analysis. The combination of intensity histogram and TS-based features from each color channel has been reported to perform very well for WCE normal-abnormal image classification in [18], but on a very small dataset. Color histograms were also combined with the statistics of discrete wavelet transformations (DWT) to detect lesions in a multiple-scale framework [19], and with LBP-based histograms to detect bleeding [8].

Shape-based image features have also been reported in endoscopic image analysis, e.g., ellipses approximating contours for polyps detection [20]. Edge orientation histograms as part of MPEG-7 visual descriptors, together with color and texture features such as dominant color and homogeneous texture, have recently been used for Crohn disease classification [3].

3. METHODOLOGY

Our normal-abnormal frame classification method consists of three steps: *feature extraction*, *feature selection* and *classification*. After feature extraction (Sections 3.1, 3.2), a feature selection method, the F-Score [21], is applied to identify the most discriminative features. Finally, these features are used for training an SVM classifier. This section focuses on feature extraction. We introduce two different methods, based respectively on image patches and scale-space, to encode statistical features at intermediate-scale image regions.

3.1. Patch-based method

Figure 2 shows the architecture of this method. An image is firstly divided into square, overlapping regions (patches). Statistics (e.g., histogram, contrast, energy; see Section 4.3 for details) of local features are then computed within each patch. To obtain a feature descriptor for the whole image, one could just concatenate all such patch-based descriptors. However this would produce high-dimensional feature vector, requiring dimensionality reduction hence additional computations. Moreover, a concatenated descriptor would implicitly encode absolute locations of features in the image, largely irrelevant for CIA and so potentially confusing for classifiers (Section 1). To avoid these problems, we compute mean and stdev of each component of the patch-based feature descriptors over all patches. As a result, the concatenation of the statistics of each descriptor component can represent intermediate-scale information appearing in image patches, without encoding spatial location information of features. In addition, the statistics (e.g., histogram) of local features (therefore at smaller scale) over the whole image are computed as global features and then concatenated with the intermediate-scale statistics to generate the final image descriptor.

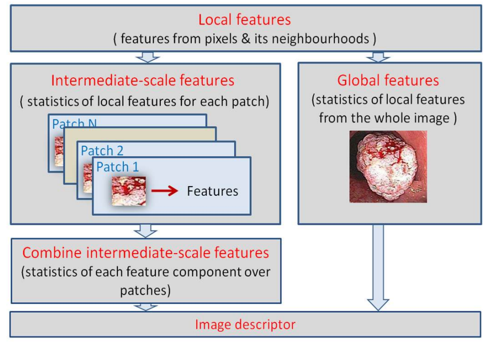

Fig. 2. Architecture of our patch-based method.

3.2. Scale-space method

A Gaussian scale-space method is used. As shown in Figure 3(b), local features are first computed from the original image and the two downscaled images respectively. Then the statistics (e.g., histogram) of local features from each of the three images are concatenated to form an image descriptor. Multi-scale image representations are well known in computer vision [22], but the method we use to extract and concatenate the statistical features, to our best knowlegde, is novel for CIA. Compared to the patch-based method which captures intermediate-scale information from the statistics of local features over image patches in the original image (Figure 3(a)), the scale-space method captures the intermediate-scale information from statistics of local features in the two downscaled images.

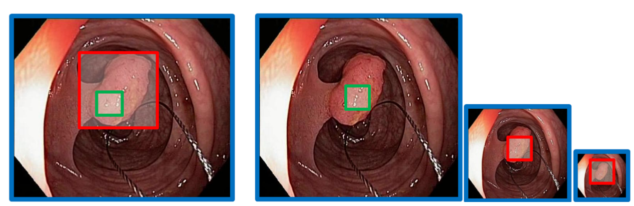

(a) Patch based method (b) Scale-space method

Fig. 3. Illustration of our two methods. (a) Statistics of local features (green) from each image patch (red) are extracted as intermediate-scale information. (b) Local features (red) in the down-sampled images capture intermediate-scale information.

Multi-resolution local binary patterns. Notice that any local features could be used in the two methods presented. In both, we use multi-resolution LBP (mLBP) as they prove robust to noise and illumination changes [4]. Figure 4 shows the local neighborhood which is quantized radially to three different radii, and, at each radius, into eight circles. An mLBP code is constructed by sampling the neighborhood at the centers of the solid circles, after a Gaussian filter with σ proportional to the radius of the circled area is applied to each circle's center.

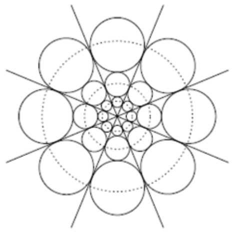

Fig. 4. Multi-resolution LBP as given in [4].

4. EXPERIMENTS

4.1. Experimental setup

82 air colonoscopy videos with varying resolutions and illumination were collected from the Internet (mainly from [23]) under clinical guidance, with abnormal videos containing frames showing various lesions or bleedings. To select a representative subset of frames from each video to be used in experiments, K-means was applied to form frame clusters based on color statistics (mean, standard deviation, skewness, kurtosis and entropy in RGB channels) and texture features (LBP histogram). One frame per cluster is selected for the final dataset. In total 1050 normal and 1050 abnormal frames were selected under clinical guidance, and rescaled to 300×300 resolution. Some examples are shown in Figure 1, and the whole dataset will be made online available soon.

All experiments were repeated 25 times and results were averaged. In each run, 500 normal and 500 abnormal images were randomly selected for training and the remainder was used for testing. SVM parameters were learned in each run using 5-fold cross validation. A SVM [24] with a RBF kernel was used for classification except being mentioned specifically.

4.2. Comparison of baseline features with multi-resolution LBP

As baseline for comparison we implemented most features reported in the endoscopy literature, including CWC [6], CWC with higher order statistics (*CWC2*) [7], GLCM on wavelet bands (*WGLCM*) [5], color histogram (*CH*) [10], texture spectrum (*TS*) [9], and local binary patterns (LBP) [8]. Compared to only one distance for GLCM and one radius for TS used in the related endoscopy literature, we tried different distances $\{1, 2\}$ for GLCM (4 directions, symmetric) and and different radii $\{1, 2\}$ for LBP and report here the best performance. To be consistent with the literature, features were computed from each color channel of the RGB color space.

A three-resolution LBP was used as local feature with radii = $\{1, 2.43, 5.44\}$. 8-bit patterns were considered for each resolution. Following [4], Gaussian filters of $\{(size = 3, \sigma = 0.38), (size = 7, \sigma = 0.85)\}$ were applied for the 2^{nd} and 3^{rd} resolutions respectively; the first resolution level is the un-smoothed original image. From each color channel in RGB space, a uniform LBP histogram was obtained at each LBP resolution, leading to a feature vector of size 531 (3 colors $\times$ 3 resolutions $\times$ 59 histogram bins).

Table 1 shows that mLBP performs significantly better (about 94%) than all the other local features (74% - 91%). One possible reason is that mLBP captures large local neighborhoods 15×15 and is robust to noise. Adding color features such as histograms to the mLBP gives small improvements ($< 0.4\%$), indicating that mLBP might capture discriminative color information as well.

Table 1. Comparison of baseline features with mLBP. F: feature, A: accuracy=(TP+TN)/all. Interval: mean $\pm$ stdev.

F	CWC	CWC2	WGLCM	CH	TS	LBP	mLBP
A	74.33 $\pm$0.88	77.01 $\pm$1.17	74.25 $\pm$1.29	83.22 $\pm$1.08	84.86 $\pm$1.41	90.74 $\pm$0.89	**94.06 $\pm$0.96**

Table 2. Accuracy improvements with intermediate-scale features. Intervals: mean $\pm$ stdev.

method	feature		
	mLBP	GLCM	Color
stats of local features	**94.06$\pm$0.96**	82.47 $\pm$ 1.34	80.09 $\pm$ 1.38
patch-based	**95.47$\pm$0.86**	86.32 $\pm$ 1.29	86.33 $\pm$ 1.26
scale-space	**95.40$\pm$0.77**	86.63 $\pm$ 1.10	83.17 $\pm$ 1.17

4.3. Evaluations of the proposed methods

For the patch-based method, three candidate window sizes, $w = \{60, 80, 100\}$ pixels, were used. For the scale-space method, three candidate maximum levels $\{1, 2, 3\}$ were used. a Gaussian filter with standard deviation 1.5 pixels was incrementally applied to obtain the images at different scales. The mLBP, GLCM, and pixel color were respectively used as local features in each method. To compute intermediate-scale features, we used histograms for mLBP, statistics including correlation, contrast, homogeneity, and energy for GLCM, and statistics including mean, std, skewness, kurtosis, and entropy for color. Cross validation found that window size 60 gave the best accuracy for the patch-based method and 3-level Gaussian scale-space gave the best accuracy for the scale-space method. For both methods, two different F-Score threshold values (0.05 and 0.01) were tested. Feature selection helps to improve classification efficiency by reducing redundancy (or the number) of features, without reducing accuracy performance (not shown due to limited space).

Table 2 shows that the two proposed methods (last two rows in Table 2) perform comparatively well and clearly better than the traditional method (without considering intermediate-scale information; first row in Table 2), regardless of the types of local features. While the proposed methods get more than 3% improvements in accuracy compared to traditional method when using the statistical features obtained from GLCM and pixel color, the accuracy is improved only by 1.4% when using the mLBP. This may be because mLBP has partially captured intermediate-scale information from the large neighborhoods. All the evidence shows that adding intermediate-scale features considerably improves the classification accuracy.

4.4. Performance of state-of-the-art features

The following features were also evaluated with dense SIFT features: bag of words (*BOW*), BOW with spatial pyramid matching (*BowSPM*) [11], sparse coding (*SC*), SC with spatial pyramid matching (*ScSPM*) [12], locally constraint linear coding (*LLC*) [13], and LLC with spatial pyramid matching (LlcSPM) [13]. For BOW and BowSPM, a SVM with χ^2 kernels was used from the publicly available library *VLFeat* [25]. The considered numbers of words were 100, 500, 1000, 2000, 4000. A three-level pyramid was used for BowSPM. For SC, ScSPM, LLC, and LlcSPM, the code available online was adopted [13, 12]. Different numbers of bases (100, 500, 1000, 2000, 4000) were tried and the best performances are reported. For LLC and LlcSPM, very small (10^{-4}) regularization parameter

Table 3. Comparison of state-of-the-art feature representations (mean and stdev).

F	BOW	BowSPM	SC	ScSPM	LLC	LlcSPM
A	86.98 $\pm$0.76	89.44 $\pm$0.73	89.86 $\pm$0.81	90.58 $\pm$0.73	88.00 $\pm$0.70	91.38 $\pm$0.92

gave the best results. Due to the computational time of SC and ScSPM, only three values of the regularization parameters (0.1,0.2,0.3) were tried. A three-level pyramid was used for ScSPM and LlcSPM. For LLC and LlcSPM the number of local coordinates was changed to 5,10, 50,100. For all the feature representations, dense SIFT features were computed as local features from 16×16 patches at 8 pixel intervals in each color RGB channel.

Table 3 shows the best accuracies obtained from the state-of-the-art features. Number of bases 4000 gave the best accuracies in all the cases. Importantly, adding spatial pyramid features with BOW, SC, or LLC consistently improves the performance, showing the importance of intermediate-scale features in frame classification. In addition, comparing the results from Tables 3 and 2, it is clear that the two methods proposed outperform considerably state-of-the-art features, probably by disregarding irrelevant spatial location information and capturing discriminative intermediate-scale features.

5. CONCLUSIONS

We proposed two methods to encode intermediate-scale information for CIA, and showed a considerable accuracy improvement regardless of the features used. We showed that encoding statistics of intermediate-scale features, in addition to the statistics of local features, improves considerably the performance of normal-abnormal classification in CIA. The experimental comparison showed the proposed representational schemes and the mLBP outperformed features adopted in reported work on CIA as well as computer vision. Future work will address tests on larger datasets, the use of temporal (video) information, exploration of further feature selection techniques, and tests on unseen video dataset (i.e., training on the images obtained from one set of videos and testing on the images from a different set of videos).

6. ACKNOWLEDGEMENT

This work is funded by 2011-2016 EU FP7 ERC project "CODIR: colonic disease investigation by robotic hydrocolonoscopy", collaborative between the Universities of Dundee (PI Prof Sir A Cuschieri) and Leeds (PI Prof A Neville). Thanks to CVIP members for comments on previous drafts.

References

[1] "Cancer research uk," `info.cancerresearchuk.org/cancerstats`.

[2] M. B. Wallace, "Improving colorectal adenoma detection: technology or technique?," *Gastroenterology*, vol. 132, pp. 1221–3, 2007.

[3] R. Kumar, Q. Zhao, S. Seshamani, G. Mullin, G. Hanger, and T. Dassopoulos, "Assessment of crohn's disease lesions in wireless capsule endoscopy images," *BioMed. Eng. online*, vol. 59, 2012.

[4] T. Mäenpää, *The Local Binary Pattern Approach to Texture Analysis: Extensions and Applications*, Acta Universitatis Ouluensis: Technica. Oulun yliopisto, 2003.

[5] D. E. Maroulis, D. K. Iakovidis, S. A. Karkanis, and D. A. Karras, "CoLD: a versatile detection system for colorectal lesions in endoscopy video-frames," *CMPB*, vol. 70, pp. 151–166, 2003.

[6] S. A. Karkanis, D. K. Iakovvidis, D. E. Maroulis, D. A. Karras, and M. Tzivras, "Computer aided tumor detection in endoscopic video using color wavelet features," *T-ITB*, vol. 7, 2003.

[7] C. S. Lima, D. Barbosa, A. Ramos, A. Tavares, L. Montero, and L. Carvalho, "Classification of endoscopic capsule images by using color wavelet features, higher order statistics and radial basis functions," in *EMBS*, 2008.

[8] B. Li and M. Meng, "Computer-aided detection of bleeding regions for capsule endoscopy images," *TBME*, vol. 56, pp. 1032–1039, 2009.

[9] V. S. Kodogiannis and M. Boulougoura, "Neural network-based approach for the classification of wireless-capsule endoscopic images," in *IJCNN*, 2005.

[10] P. C. Khun, Z. Zhuo, L. Z. Yang, L. Liyuan, and L. Jiang, "Feature selection and classification for wireless capsule endoscopic frames," in *ICBPE*, 2009.

[11] S. Lazebnik, C. Schmid, and J. Ponce, "Beyond bags of features: Spatial pyramid matching for recognizing natural scene categories," in *CVPR*, 2006.

[12] J. Yang, K. Yu, Y. Gong, and T. Huang, "Linear spatial pyramid matching using sparse coding for image classification," in *CVPR*, 2009.

[13] J. Wang, J. Yang, K. Yu, F. Lv, T. Huang, and Y. Gong, "Locality-constrained linear coding for image classification," in *CVPR*, 2010.

[14] T. Ojala, M. Pietikinen, and D. Harwood, "Performance evaluation of texture measures with classification based on kullback discrimination of distributions," in *ICPR*, 1994.

[15] Q. Zhao and M. Q. H. Meng, "Polyp detection in wireless capsule endoscopy images using novel color texture features," in *WCICA*, 2011.

[16] S. Engelhardt, S. Ameling, D. Paulus, and S. Wirth, "Features for classification of polyps in colonoscopy," in *CEUR Workshop*, 2010.

[17] Y. Lee and G. Yoon, "Bleeding detection algorithm for capsule endoscopy," in *WASET*, 2011.

[18] M. P. Tjoa and S. M. Krishnan, "Feature extraction for the analysis of colon status from the endoscopic images," *BioMed. Eng. online*, 2003.

[19] P. Li, K. L. Chan, and S. M. Krishnan, "Learning a multi-size patch-based hybrid kernel machine ensemble for abnormal region detection in colonoscopic images," in *CVPR*, 2005.

[20] S. Hwang, J. H. Oh, W. Tavanpong, J. Wong, and P. C. Groen, "Polyp detection in colonoscopy video using elliptical shape feature," in *ICIP*, 2007.

[21] Y. W. Chen and C. J. Lin, "Combining svms with various feature selection strategies," in *Feature extraction, foundations and applications*, 2006.

[22] T. Lindeberg, "Scale-space theory: A basic tool for analysing structures at different scales," *Journal of Applied Statistics*, pp. 224–270, 1994.

[23] "Gastrolab- the gastrointestinal site," `http://www.gastrolab.net/`.

[24] C. C. Chang and C. J. Lin, "LIBSVM: A library for support vector machines," *ACM TIST*, vol. 2, 2011.

[25] A. Vedaldi and B. Fulkerson, "VLFeat: An open and portable library of computer vision algorithms," 2008.